MOLECULAR AND CELLULAR BIOLOGY, Dec. 1992, p. 5736–5747
0270-7306/92/125736-12$02.00/0

Vol. 12, No. 12

CTF4 (*CHL15*) Mutants Exhibit Defective DNA Metabolism in the Yeast *Saccharomyces cerevisiae*

N. KOUPRINA,[1,2] E. KROLL,[1,2] V. BANNIKOV,[3] V. BLISKOVSKY,[3] R. GIZATULLIN,[3] A. KIRILLOV,[3] V. ZAKHARYEV,[3] P. HIETER,[2] F. SPENCER,[2] AND V. LARIONOV[1]†*

Institute of Cytology, Academy of Sciences of Russia, St. Petersburg 194064,[1] and V. A. Engelhardt Institute of Molecular Biology, Academy of Sciences of Russia, Moscow 117984,[3] and Department of Molecular Biology and Genetics, Johns Hopkins Medical School, Baltimore, Maryland 21205[2]

Received 22 May 1992/Returned for modification 16 July 1992/Accepted 28 September 1992

We have analyzed the *CTF4* (*CHL15*) gene, earlier identified in two screens for yeast mutants with increased rates of mitotic loss of chromosome III and artificial circular and linear chromosomes. Analysis of the segregation properties of circular minichromosomes and chromosome fragments indicated that sister chromatid loss (1:0 segregation) is the predominant mode of chromosome destabilization in *ctf4* mutants, though nondisjunction events (2:0 segregation) also occur at an increased rate. Both inter- and intrachromosomal mitotic recombination levels are elevated in *ctf4* mutants, whereas spontaneous mutation to canavanine resistance was not elevated. A genomic clone of *CTF4* was isolated and used to map its physical and genetic positions on chromosome XVI. Nucleotide sequence analysis of *CTF4* revealed a 2.8-kb open reading frame with a 105-kDa predicted protein sequence. The *CTF4* DNA sequence is identical to that of *POB1*, characterized as a gene encoding a protein that associates in vitro with DNA polymerase α. At the N-terminal region of the protein sequence, zinc finger motifs which define potential DNA-binding domains were found. The C-terminal region of the predicted protein displayed similarity to sequences of regulatory proteins known as the helix-loop-helix proteins. Data on the effects of a frameshift mutation suggest that the helix-loop-helix domain is essential for *CTF4* function. Analysis of sequences upstream of the *CTF4* open reading frame revealed the presence of a hexamer element, ACGCGT, a sequence associated with many DNA metabolism genes in budding yeasts. Disruption of the coding sequence of *CTF4* did not result in inviability, indicating that the *CTF4* gene is nonessential for mitotic cell division. However, *ctf4* mutants exhibit an accumulation of large budded cells with the nucleus in the neck. *ctf4 rad52* double mutants grew very slowly and produced extremely high levels (50%) of inviable cell division products compared with either single mutant alone, which is consistent with a role for *CTF4* in DNA metabolism.

The eukaryotic chromosome cycle, which includes the coordination and execution of replication and segregation of chromosomes within the mitotic cell division cycle, is currently under intensive study. *Saccharomyces cerevisiae* is an excellent organism for the study of the mitotic chromosome cycle because of its accessibility to genetic and molecular techniques. All of the *cis*-acting DNA elements involved in chromosome replication and segregation, including origins of replication, telomeres, and centromeres, in yeasts have been identified (for a review, see references 4, 7, 34, and 55). In addition, many *trans*-acting genes important for execution of the mitotic chromosome cycle in yeasts have been described, including genes required for metabolic maintenance and replication of chromosomal DNA (e.g., polymerase subunits [2, 16, 29] and enzymes that carry out precursor synthesis [54]), genes that participate in the organization of chromatin (e.g., histones [25]), and genes that encode components of the segregational machinery (e.g., tubulins [33, 41] and candidate motor proteins [26]).

Our laboratories have recently described collections of mutants with impaired mitotic chromosome transmission, *ctf* and *chl* mutants (17, 19, 46). *ctf* mutants (for chromosome transmission fidelity) have been selected by using a visual color assay to monitor the inheritance of an artificially generated nonessential marker chromosome. *chl* mutants (for chromosome loss) have been identified by using the criteria for chromosome III and circular artificial minichromosome instability. The criteria used for selection of *ctf* and *chl* mutants were expected to define new genes controlling both chromosome segregation and replication in yeasts. It has been shown recently that most *chl* mutations complement *ctf* mutations (18), so these two collections appear to increase the spectrum of potentially new genes. A third similar collection, the *cin* mutants (for chromosome instability), has also been described (13).

At present, yeast genomic DNAs that complement mutations in eight *ctf* and five *chl* strains have been obtained from clones. One of the genes, *CTF1*, has been analyzed in more detail (10). It was shown that *CTF1* is identical to the previously identified *CHL1* gene (22) and encodes a 99-kDa predicted protein homologous to the coding region of a nucleotide excision repair yeast gene, *RAD3* (49). Domains of homology between these two predicted protein sequences included a helix-turn-helix (HTH) motif and an ATP binding site. Mutants lacking the *CTF1* gene product are viable and display an increased frequency of both chromosome III loss and nondisjunction and a delay in cell cycle progression in G2/M.

We present genetic and molecular analyses of the *CTF4* gene, which has been identified in both the *ctf* and *chl* mutant sets. *CTF4* was isolated independently by Miles and Formosa as a gene encoding a DNA polymerase α-binding protein (*POB1* [27]). Both this study and that described by

* Corresponding author.
† Present address: National Institute of Environmental Health Sciences, P.O. Box 12233, Research Triangle Park, NC 27709.

TABLE 1. Strains used in this study

S. cerevisiae strain	Genotype	Source or reference
CL15-1	*MATα/MATa leu2-1/leu2-27 his4/HIS4 thr4/THR4 ade2 met2 ura3-52 chl15-1*	This study
Z4221-3c1	*MATα/MATa leu2-1/leu2-27 his4/*HIS4 *thr4/THR4 ade2 met2 ura3-52*	J. Roth
YNK34[a]	*MATα chl15-1 ade2-101 ura3-52 his3Δ200 leu2Δ1* + CFIII(CEN3.L.YPH278)*URA3 SUP11*	This study
YNK35[a]	*MATa chl15-1 ade2-101 ura3-52 trp1Δ1 his4 leu2Δ1* + CFIII(CEN3.L.YPH278)*URA3 SUP11*	This study
YNK36	*Diploid derived from YNK34 × YNK35*	This study
CL15	*MATa leu2-27 ade2 met2 ura3-52 chl15-1*	18
CL15α	*MATα his4 leu2-1 thr4 ade2 met2 ura3-52 chl15-1*	18
YNK27[b]	*MATα leu2-1 his4 thr4 ade2 met2 ura3-52*	This study
YNK28[b]	*MATa leu2-27 ade2 met2 ura3-52*	This study
YNK29[c]	*MATα/MATa leu2-1/leu2-27 his4/HIS4 thr4/THR4 ade2/ade2 met2/met2 ura3-52/ura3-52*	This study
YNK30[c]	*MATα/MATa leu2-1/leu2-27 his4/HIS4 thr4/THR4 ade2/ade2 met2/met2 ura3-52/ura3-52 chl15-1/chl15-1*	This study
YPH98	*MATa ura3-52 lys2-801 ade2-101 trp1Δ1 leu2Δ1*	46
YPH102	*MATα ura3-52 lys2-801 ade2-101 his3Δ200 leu2Δ1*	46
YPH501	*MATα/MATa leu2Δ1/leu2Δ1 his3Δ200/his3Δ200 trpΔ63/trpΔ63 ade2-101/ade2-101 lys2-801/lys2-801 ura3-52/ura3-52*	This study
YPH278	*MATα ura3-52 lys2-801 ade2-101 his3Δ200 leu2Δ1* + CFIII(CEN3.L.YPH278)*URA3 SUP11*	46
YPH926	*MATa ura3-52 lys2-801 ade2-101 his3Δ200 trp1Δ63 leu2Δ1*	This study
YPH927	*MATα ura3-52 lys2-801 ade2-101 his3Δ200 trp1Δ63 leu2Δ1*	This study
YPH928	*MATα ura3-52 lys2-801 ade2-101 his3Δ200 trp1Δ63 leu2Δ1 ctf4Δ3::URA3*	This study
YPH929	*MATa ura3-52 lys2-801 ade2-101 his3Δ200 trp1Δ63 leu2Δ1 ctf4Δ3::URA3*	This study
YPH930	*MATα/MATa leu2Δ1/LEU2 his3Δ200/hisΔ200 trpΔ63/trpΔ63 ade2-101/ade2-101 lys2-801/lys2-801 ura3-52/ura3-52*	This study
YPH931	*MATα/MATa leu2Δ1/LEU2 his3Δ200/his3Δ200 trpΔ1/trpΔ63 ade2-101/ade2-101 lys2-801/lys2-801 ura3-52/ura3-52 ctf4Δ3::URA3/ctf4Δ3::URA3* + CFVII(RAD2.d.YPH877)*TRP1 SUP11*	This study
YPH932	*MATα/MATa leu2Δ1/leu2Δ1 his3Δ200/HIS3 TRP1/trpΔ1 ade2-101/ade2-101 lys2-801/lys2-801 ura3-52/ura3-52 ctf4-50/ctf4-107* + CFVII(RAD2.d.YPH877)*TRP1 SUP11*	46
YPH933	*MATα/MATa leu2Δ1/leu2Δ1 his3Δ200/HIS3 TRP1/trpΔ1 ade2-101/ade2-101 lys2-801/lys2-801 ura3-52/ura3-52 ctf4-25/ctf4-107* + CFVII(RAD2.d.YPH877)*TRP1 SUP11*	46
YPH934	*MATa ura3-52 lys2-801 ade2-101 trp1Δ1 leu2Δ1 ctf4-107 his4*::pV100(*URA3*)	This study
YPH935	*MATa ura3-52 lys2-801 ade2-101 trp1Δ1 leu2Δ1 his4*::pV100(*URA3*)	This study
YPH936	*MATα ura3-52 lys2-801 ade2-101 his3Δ200 trp1Δ63 leu2Δ1 rad52Δ1::URA3*	This study
YPH937	*MATα ura3-52 lys2-801 ade2-101 trp1Δ1 leu2Δ1 ctf4Δ1::TRP1*	This study
YPH938	*MATa ura3-52 lys2-801 ade2-101 his3Δ200 trp1Δ1 leu2Δ1 ctf4Δ1::TRP1 rad52Δ1::URA3*	This study
YCTF25	*MATα ura3-52 lys2-801 ade2-101 leu2Δ1 his3Δ200 ctf4-25*	
YCTF41	*MATα ura3-52 lys2-801 ade2-101 leu2Δ1 his3Δ200 ctf4-41* + CFIII(CEN3.L.YPH278)*URA3 SUP11*	46
YCTF43	*MATα ura3-52 lys2-801 ade2-101 leu2Δ1 his3Δ200 ctf4-43* + CFIII(CEN3.L.YPH278)*URA3 SUP11*	46
YCTF46	*MATα ura3-52 lys2-801 ade2-101 leu2Δ1 his3Δ200 ctf4-46* + CFIII(CEN3.L.YPH278)*URA3 SUP11*	46
YCTF50	*MATα ura3-52 lys2-801 ade2-101 leu2Δ1 his3Δ200 ctf4-50* + CFIII(CEN3.L.YPH278)*URA3 SUP11*	46
YCTF65	*MATα ura3-52 lys2-801 ade2-101 leu2Δ1 his3Δ200 ctf4-65* + CFIII(CEN3.L.YPH278)*URA3 SUP11*	46
YCTF66	*MATα ura3-52 lys2-801 ade2-101 leu2Δ1 his3Δ200 ctf4-66* + CFIII(CEN3.L.YPH278)*URA3 SUP11*	46
YCTF107	*MATa ura3-52 lys2-801 ade2-101 leu2Δ1 trp1Δ1 ctf4-107* + CFVII(RAD2.d.YPH277)*URA3 SUP11*	46
YCTF154	*MATa ura3-52 lys2-801 ade2-101 leu2Δ1 trp1Δ1 ctf4-154* + CFVII(RAD2.d.YPH362)*URA3 SUP11*	46

[a] These strains, carrying the chromosome fragment CFIII(CEN3.L.YPH278)*URA3 SUP11*, were generated by standard genetic methods from crosses between CL15 strains and YPH278.

[b] Haploid mitotic segregant of Z4221-3cl, which is disomic for chromosome III.

[c] Isogenic strains YNK29 and YNK30 were obtained by crossing haploid mitotic segregants *MAT*a and *MAT*α of disomic Z4221-3cl and CL15-1, respectively.

Miles and Formosa indicate a critical role for *CTF4* in chromosome transmission and suggest that the *CTF4* gene product is involved in DNA metabolism.

MATERIALS AND METHODS

Strains and media. The yeast strains used in this study are listed in Table 1. The *ctf4-Δ1::TRP1* mutation was constructed in vitro as follows. A 2.2-kb *Cla*I-*Sph*I fragment of the *CTF4* gene (from the *Cla*I site at position +404 to the *Sph*I site at position +2621) was cloned into pBR325. The 0.3-kb *Eco*RI fragment (from the *Eco*RI site at position +671 to the *Eco*RI site at position +944) was deleted and substituted with a 1.45-kb *Eco*RI fragment containing the *TRP1* gene (50), yielding plasmid YIp10. This plasmid was digested with *Cla*I and *Sph*I, giving a 3.4-kb fragment containing the *ctf4-Δ1::TRP1* allele and used to replace the wild-type *CTF4* gene by one-step gene replacement (39), thus creating YPH937. The mutant allele has a 273-bp deletion which corresponds to 91 amino acid residues of the internal region of the *CTF4* predicted protein. This deletion interrupts the open reading frame at the 223rd codon. The *ctf4Δ3::URA3* mutation was constructed by cutting p37 with *Mlu*I and *Sph*I, blunting the ends with T4 polymerase, and inserting a 1.4-kb *Sma*I-*Sma*I fragment containing the *URA3* gene (isolated from a subclone of the *Hin*dIII-*Hin*dIII *URA3*-containing fragment in pRS315). This plasmid was digested with *Xba*I and used to replace the wild-type *CTF4* gene by one-step gene replacement (39). In *ctf4Δ3::URA3*, all but the last 167 bp of the *CTF4* open reading frame have been deleted.

The following manipulations resulted in an isogenic group of strains used to study *ctf4 rad52* double mutants. Introduction of the *rad52-Δ1::URA3* deletion in YPH927 (*CTF4*) was carried out by one-step gene disruption with a 3,141-bp *Sph*I-*Sal*I fragment of the pDU1 plasmid. (In pDU1, the

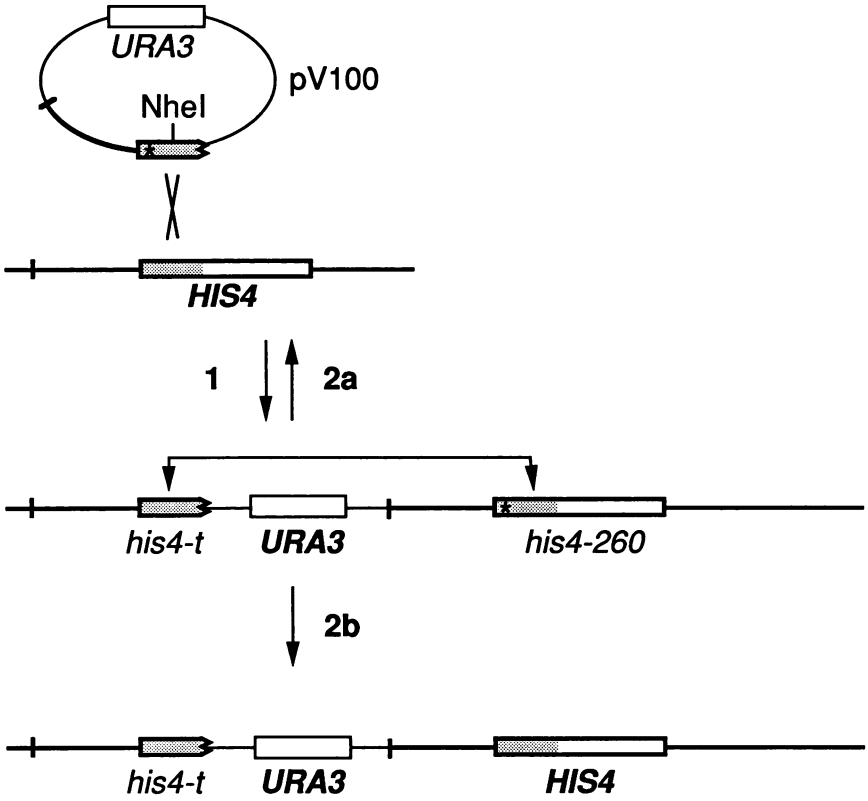

FIG. 1. Assay for intrachromosomal mitotic reciprocal recombination and gene conversion. pV100 contains 2.8 kb of yeast genomic DNA, including the promoter region and about 500 bp of coding sequence from *his4-260* (a missense mutation indicated by the asterisk). Targeted integration (labeled "1") of this plasmid (via linearization at the *Nhe*I site) results in the introduction of a 3'-truncated copy of the *HIS4* locus (labeled *his4-t*) and a *his4-260* complete gene copy, separated by the *URA3*-containing plasmid vector. His^+ segregants can arise from reciprocal recombination between the direct repeats (either intrastrand or due to unequal sister chromatid exchange, labeled "2a") or from gene conversion of the missense allele to the wild type (labeled "2b"). Reciprocal recombination events are distinguished from gene conversion events by the loss of the *URA3* marker.

major part of the *RAD52* reading frame between the *Bst*EI and *Pst*I sites is replaced by the 2,058-bp *Bcl*I-*Bam*HI *URA3* gene fragment from plasmid pBR325-*URA3*. The plasmid was kindly provided by Ed Perkins.) The resulting strain YPH936 (*rad52Δ1::URA3 CTF4*) was crossed to YPH937 (*RAD52 ctf4Δ1::TRP1*), the diploid was sporulated, and tetrads were dissected. A Trp^+ Ura^+ spore clone (YPH938) was chosen for further study.

To construct YPH934 [*ctf4-107 his4*::pV100(*URA3*)], pV100 (kindly provided by S. Roeder) was linearized with *Nhe*I and used to transform a red segregant from YCTF107 (*ctf4-107*). pV100 contains a 2.8-kb *Eco*RI-*Sal*I-*Sal*I fragment of *his4-260* (including about 500 bp of the coding sequence) inserted between the *Eco*RI and *Sal*I sites of YIp5. *his4-260* contains a missense mutation located ~200 bp from the *Nhe*I site, which is ~230 bp from the 3'-most *Sal*I site. Independent Ura^+ transformants were screened for a His^- phenotype that papillated to His^+, indicating that the integrating recombination event indeed occurred in *HIS4* DNA between the point mutation (*his4-260*) and the 3' truncation, as shown in Fig. 1. This arrangement in the genome was confirmed by Southern analysis (data not shown). The isogenic wild-type control was generated similarly, starting with YPH98 (*CTF4*).

Standard media recipes (43) were used, with exception of the concentration of supplemental adenine, which was added at a low concentration to enhance the development of red pigment by *ade2-101* cells (12). Genetic analysis was performed by using standard protocols (43) for mating, diploid selection, sporulation, and tetrad dissection. Yeast transformation was performed by the LiCl procedure of Ito et al. (15).

Chromosome segregation and recombination assays. Quantitative measurements of the frequencies of cells derived from chromosome III loss and recombination (17) and the frequency of centromeric plasmid loss per generation (37) were performed as previously described. Genotypes of the strains characterized are found in Table 1 (Z4221-3c1 for *CTF4* and CL15-1 for *ctf4-1* [*chl15-1*]).

Strains YPH930, -931, -932, and -933 have either the genetically marked chromosome fragment CFVII(RAD2.d.YPH362) *URA3 SUP11* (46) or CFVII(RAD2.d.YPH877)*TRP1 SUP11* (10). The presence of the suppressor tRNA gene *SUP11* on these marker chromosomes makes it possible to visualize the fragments' mitotic stability by appearance of red and white sectors within pink colonies in an *ade2-101* (ochre) genetic background. Half-sector analysis was used to measure rates of chromosome fragment loss and nondisjunction as described previously (12).

Fluctuation analysis. Fluctuation analysis was used to determine the rates of rare events in two assays. In the first, rates of intrastrand reciprocal exchange and gene conversion at the *his4::pV100*(*URA3*) loci in YPH934 and YPH935 were measured. Ten independent test colonies were removed

from YPD on agar plugs and suspended in 1 ml of sterile H_2O. Appropriate dilutions were plated on YPD (to determine the number of viable cells) and minimal media lacking histidine (to determine the number of His^+ cells per test colony). Uracil prototrophy or auxotrophy of these His^+ cells was determined by replica plating. Rates were calculated separately from the median frequencies of His^+ Ura^- (reciprocal exchange) and His^+ Ura^+ (gene conversion) cells by using the method of the median (20). Rates of spontaneous mutation to canavanine resistance were similarly measured, but with six to nine test colonies per genotype.

Cloning of the *CTF4* gene. *CTF4* was cloned from a library (46a) of 10- to 12-kb fragments of yeast genomic DNA inserted into pBR322-based *LEU2 CEN4 ARS1* shuttle vector pSB32 (49a). Putative *CTF4*-containing clones were identified by screening Leu^+ transformants of YNK36 (*ctf4-1 leu2Δ1*) for complementation of the sectoring phenotype. These occurred at a frequency of 1 in 3,000 transformants. Plasmids were rescued in *Escherichia coli* by transformation of yeast genomic DNA preparations. To subclone the gene within the cloned DNA segments, the smallest of the five genomic clones obtained, F12, was partially digested with *Sau*3A and 3- to 5-kb fractions were agarose gel purified and shotgun cloned into the *Bam*HI site of pBLUESCRIPT-based *CEN6 LEU2 ARSH4* shuttle vector pRS315 (45). *CTF4*-complementing subclones were identified by the ability to complement the sectoring phenotype of the *ctf4-1* mutant. Deletion and insertion mutageneses on the smallest of these pRS315-based *CTF4* subclones (p37) were performed by using complete or partial digestion of the plasmid with various restriction enzymes and subsequent ligation with T4 DNA ligase.

Proof that the cloned DNA corresponds to the *CTF4* locus was obtained as follows. The *CTF4* gene was marked with *LEU2* by integrative transformation of a wild-type strain (YNK27) with a *LEU2 CTF4* YIp plasmid (pRS305 containing the 4-kb *Xba*I fragment of p37) that had been linearized within the *CTF4* sequence at the *Mlu*I site. The resulting transformants did not exhibit a sectoring phenotype. A diploid was constructed by mating one of the transformants with YNK35 (*ctf4-1*) and subsequently sporulated for tetrad analysis. Of the 50 chromosome fragment-containing spores in 25 four-spored tetrads, all were either Leu^+ Chl^+ or Leu^- Chl^- (Chl^- indicates mitotic instability of the chromosome fragment and of chromosome III). These data indicated that the genomic fragment complementing the *ctf4-1* mutation corresponds to the *CTF4* gene.

Physical and genetic map positions. A physical mapping method (9) was used to map the position of *CTF4* on chromosome XVI. A 3.0-kb *Hin*dIII fragment (overlapping the *MSS18* gene and the promoter region of *CTF4*) was cloned in both orientations into the chromosome fragmentation vectors YCF3 and YCF4 (9). These constructs were linearized to reveal free ends in *CTF4* sequences and the telomere-adjacent Y′ sequences and used to transform yeast strain YPH49. Depending on the orientation of the *CTF4*-containing fragment in the vectors, stably maintained chromosome fragments were generated either with all sequences proximal to *CTF4* (acentric vector) or with all sequences distal to *CTF4* (centric vector). The sizes of these chromosome fragments were determined by orthogonal-field-alternation gel electrophoretic analysis (5).

The *CTF4* gene was placed on the phage map of the yeast genome constructed by Riles and Olson (38a) by using a 400-bp restriction fragment from *CTF4* (from the *Mlu*I site upstream of the open reading frame to the *Cla*I site within the gene) labeled with ^{32}P by random priming (8).

DNA sequencing. DNA sequencing was performed by the chain termination method (40). For sequencing of the *CTF4* gene, DNA fragments of the p37 plasmid were subcloned into M13mp18 and M13mp19 and sets of deletions were generated with exonuclease III and S1. Single-stranded M13 DNA was sequenced with the Sequenase kit (Pharmacia LKB Biotechnology) under conditions recommended by the manufacturer.

Cell cycle distribution. Yeast cells in the logarithmic growth phase were fixed, treated with RNase A, and stained with propidium iodide essentially as described in reference 14. These samples were subjected to flow cytometry with a Coulter EPICS 752 flow cytometer. Similarly prepared samples were scored for bud size and nuclear morphology by epifluorescence with a rhodamine filter set. The positively scored class was defined as very large budded cells (in which the diameter of the smaller spheroid $\geq 0.75\times$ the diameter of the larger spheroid) that had a single chromosomal mass protruding into the mother-bud neck.

Nucleotide sequence accession number. The GenBank/EMBL accession number for the primary nucleotide sequence of *CTF4* is M94769.

RESULTS

***CHL15*, *CTF4*, and *POB1* are identical.** Two lines of evidence support the idea that *CHL15*, *CTF4*, and *POB1* are identical. The first comes from complementation tests between mutant strains from the *chl* and *ctf* collections. Most *ctf* mutants (though initially isolated for chromosome fragment sectoring) also exhibit a diploid bimating phenotype (46). Since this phenotype of *chl15-1* in CL15-1 (from the *chl* collection) and a panel of representative *ctf* mutants (≥ 1 allele per *ctf* complementation group) was recessive, this property was used to determine complementation in heterozygotes. In this assay, *chl15-1* failed to complement a recessive bimating defect in six independently derived *ctf4* mutant strains (YCTF25, YCTF43, YCTF50, YCTF65, YCTF66, and YCTF154). Furthermore, the chromosome fragment sectoring phenotype of all nine *ctf4* mutant strains (YCTF46, YCTF41, YCTF107, and those listed above) was fully complemented in transformants containing a *CEN ARS* plasmid (p37) carrying a 4.5-kb restriction fragment that was isolated by complementation of the *chl15-1* mutation (described below). Thus, *ctf4* mutants fail to complement the mutation *chl15-1*, and both are complemented by the same genomic segment.

In all, there were 10 mutagenesis-induced alleles of *ctf4* recovered in the *chl* and *ctf* collections. These exhibit a large range of severity in chromosome missegregation. Qualitative scoring of the chromosome fragment sectoring phenotypes (as described in reference 46) can be used to classify mutants as rarely sectoring (YCTF107), moderately sectoring (YCTF41 and YCTF154), or frequently sectoring (YCTF25, YCTF43, YCTF46, YCTF50, YCTF65, YCTF66, and YPH931). In addition, YCTF25 and YCTF154 exhibit markedly decreased viability at 37°C (46), as does the heteroallelic diploid derived from crossing these strains (data not shown).

In the course of this work, we found that the same genetic locus has been studied as *POB1* (see below and reference 27). For simplicity in nomenclature, all three study groups have agreed to use the same name, and we will from now on refer to this locus as *CTF4*. We therefore substitute the name *ctf4-1* for the mutant allele previously described as *chl15-1*.

TABLE 2. Meiotic segregation of YCp41 minichromosome in hybrids[a]

Hybrid	No. (%) of tetrads with minichromosome marker (LEU2+) segregation[b]	
	2+:2− or 1+:3−	4+:0− or 3+:1−
YNK28[c] × GRF18 (wild type × wild type)	22 (88)	3 (12)
CL15[c] × GRF18 (*ctf4-1* × wild type)	23 (85)	4 (15)
CL3[c] × GRF18 (*chl3-1* × wild type)	13 (24)	42 (76)
CL3 × GRF18[c] (*chl3-1* × wild type)	16 (80)	4 (20)

[a] To estimate the number of minichromosomes in *chl* or *ctf* mutant cells, diploids were induced to sporulate immediately after they had been obtained, with no propagation or subcloning (17).
[b] Only tetrads containing minichromosomes were counted.
[c] Parent transformed with the minichromosome YCp41.

Chromosome instability in *ctf4* mutants is due to both chromosome loss and nondisjunction. The hypothesis that chromosome instability in *ctf4* mutants is due to both chromosome loss and nondisjunction was confirmed in two assays. In one, the copy number of the circular minichromosome YCp41 (6) in *ctf4-1* mutant cells was determined by observing its segregation in tetrads after it was mated to wild-type cells. First, the mitotic instability of YCp41 minichromosomes was assessed by measuring the frequency of minichromosome-lacking cells in selectively grown cultures as previously described (37). The measured frequencies for *CTF4* (YNK29) and *ctf4-1* (YNK30) strains were 2.0×10^{-2} and 1.5×10^{-1}, respectively, indicating a 7.5-fold increase in minichromosome loss in the mutant. If the minichromosome instability were due to an elevated level of mitotic nondisjunction (2:0 segregation of the minichromosome), an increase in average copy number in the *ctf4-1* cell population would result. Mitotic accumulation in haploid mutants can be revealed by mass mating to wild-type cells and tetrad analysis of the hybrid cells. If the hybrid population received on average more than one copy of the minichromosome from the mutant, 4+:0− and 3+:1− plasmid marker segregation will be predominant. If the hybrid received one copy of the minichromosome from the mutant, minichromosome marker segregation in the tetrads will be predominantly 2+:2− and 1+:3−. Data on the meiotic segregation of a *LEU2*-marked centromeric plasmid, YCp41 in the CL15 × GRF18 hybrid, are shown in Table 2. More than 80% of the tetrads showed 2+:2− and 1+:3− $LEU2^+$ marker segregation. In contrast, in tetrads derived from a different hybrid, CL3 × GRF18 having received the minichromosome from a mutant causing minichromosome nondisjunction (17), minichromosome marker segregation was predominantly 4+:0 and 3+:1−. By this assay there is little or no mitotic accumulation of circular minichromosomes in *ctf4-1* mutants.

We have also characterized the chromosome instability phenotype in the *ctf4-1* mutant by using a chromosome fragment, an independently segregating nonessential disomic chromosome (46). The chromosome fragment has a centromere-linked colony color marker, *SUP11* (12), allowing visual scoring of chromosome loss or gain. The tight centromere linkage of *SUP11* and the chromosome fragment centromere ensures that the loss of the *SUP11* marker indicates the loss of the chromosome and will not be due to segregation after mitotic recombination. Nondisjunction (2:0 segregation) and loss (1:0 segregation) of the chromosome fragment are revealed by the color phenotype of colony sectors. Missegregation events occurring in the first division of colony growth result in white/red (2:0) or pink/red (1:0) half-sectored colonies and provide a quantitative measurement of the rates of nondisjunction and loss. Half-sector analysis of chromosome fragment segregation in two heteroallelic mutagenesis-induced diploids (YPH932 and YPH933) and a deletion mutant (in YPH931, described in Materials and Methods and below) is shown in Table 3. Because the chromosome fragment short arms differed slightly in structure, appropriate isogenic controls are shown for each (the fragments in YPH930 and YPH931 were marked with *TRP1*; and those in YPH932, YPH933, and YPH279 were marked with *URA3*). The data indicate that the rate increase for 1:0 events in all three mutant diploids is ~300-fold, whereas that for the 2:0 events is ~50- to 230-fold. Thus, the predominant chromosome missegregation phenotype is 1:0, but both types of events occur more frequently. This suggests that chromosome destabilization occurs both by sister chromatid loss (1:0 segregation) and nondisjunction (2:0 segregation) in *ctf4* mutants.

TABLE 3. Chromosome fragment half-sector analysis: chromosome loss versus nondisjunction

Strain	Relevant genotype	No.	1:0 segregation[a]	2:0 segregation[a]
YPH930	*CTF4/CTF4*	29,800	0.04	0.01
YPH931	*ctf4Δ3/ctf4Δ3*	438	13.2	2.3
YPH279[b]	*CTF4/CTF4*	29,046	0.03	0.03
YPH932	*ctf4-50/ctf4-107*	702	8.8	2.1
YPH933	*ctf4-25/ctf4-107*	798	10	1.7

[a] Events per generation (10^2).
[b] As previously determined (10).

Mitotic recombination rates are elevated in *ctf4* mutants. The relative contributions of mitotic recombination and chromosome loss were determined by characterizing the missegregation of chromosome III markers in a disome (*MATαhis4 thr4/MATaHIS4 THR4*). The culture frequencies of cells resulting from recombination (His^- Thr^+ and His^+ Thr^-) and of cells resulting from chromosome loss (His^- Thr^- cells that mate as *MATα*) were elevated in the *ctf4-1* mutant 280- and 115-fold, respectively. (The recombination frequency for YNK29 [*CTF4*] was 8.9×10^{-5}, while that for YNK30 [*ctf4-1*] was 250×10^{-5} [19]; the missegregation frequency for YNK29 was 5.2×10^{-5}, while that for YNK30 was 600×10^{-5} [19]). Thus, both mitotic recombination between homologs and chromosome loss are increased in *ctf4* mutants.

The relative rates of intrachromosomal reciprocal recombination and gene conversion at *HIS4* were measured by fluctuation analysis of strains containing the test construct depicted in Fig. 1. In this assay, reciprocal recombination events that restore a His^+ phenotype (intrastrand or unequal sister chromatid exchange) will result in the loss of the *URA3* marker. In contrast, gene conversion events (or simple back mutations) will generate His^+ Ura^+ segregants. The rate of reciprocal recombination at *HIS4* was observed to increase 4.6-fold, whereas the gene conversion rate remained within 2-fold that of the wild type. (The reciprocal rate for YPH935 [*CTF4*] was 6.7×10^{-5}, while that for YPH934 [*ctf4-107*] was 31×10^{-5}; the gene conversion rate for YPH935 was 7.5×10^{-5}, while that for YPH934 was 12

$\times 10^{-5}$.) In our experience, multiple determinations of rates by fluctuation analysis vary within a twofold range; thus, we believe that the gene conversion rate is not significantly altered.

To summarize, the data indicate that both interchromosomal recombination (between homologs) and intrachromosomal recombination (between direct repeats) are elevated in *ctf4* mutants.

Spontaneous mutagenesis rates are not elevated in *ctf4* mutants. The identity of *CTF4* and *POB1* (by DNA sequence; see below) raised the possibility that *ctf4* mutants might exhibit defects in DNA replication or repair that would result in decreased fidelity of that process. Measurement of the rate of spontaneous mutation to canavanine resistance provides a simple method for monitoring the fidelity of replication. Five mutant haploid strains (YCTF25, YCTF43, YCTF107, YCTF154, and YPH928) were assayed by fluctuation analysis and compared with isogenic control strains (YPH98, YPH102, and YPH926). All mutated to canavanine resistance at rates within twofold those of the wild type ($\sim 3 \times 10^{-6}$), indicating that the fidelity with which chromosomal DNA is replicated in *ctf4* mutants is equivalent to that in the wild type.

Cloning of the *CTF4* gene. Plasmids containing the *CTF4* gene were identified by visual screening for complementation of the sectoring phenotype of a *ctf4-1/ctf4-1 leu2Δ1/leu2Δ1* mutant. Strain YNK36 was transformed with plasmid DNA containing a yeast genomic library of 10- to 12-kb fragments inserted into an *ARS1 CEN4 LEU2*-based vector. Leu^+ transformants giving rise to homogeneously pink (nonsectoring) colonies were candidates for yeast cells containing a genomic clone of *CTF4*. Plasmid DNA was recovered in *Escherichia coli* from five independent transformants. Restriction fragment analysis indicated that all five plasmids contained overlapping but not identical inserts. All five recovered plasmids rescued the *ctf4-1* sectoring phenotype, minichromosome instability, and chromosome III loss upon retransformation and therefore contained a *ctf4-1* complementing genomic segment. The smallest of five clones contained a 10-kb genomic insert, and the plasmid containing this fragment (F12) was used for subsequent analysis. The location of *CTF4* was further defined by constructing a library of 3- to 5-kb fragments generated by partial *Sau*3A digestion of F12 in the multipurpose vector pRS315 (*CEN6 ARSH4 LEU2*). Plasmid p37 contained a 4.5-kb insert and fully complemented the *ctf4-1* mutant phenotypes. Various subclones of this insert (p37/1 to p37/7) were constructed and tested for complementing activity (Fig. 2). p37/4 exhibited only partial complementation of *ctf4-1*; obtained transformants exhibited an intermediate sectoring phenotype, and the mitotic stability of plasmid p37/4 in the transformants was intermediate (70%) compared with its stability in the wild-type strain (90%) and in mutant *ctf4-1* (50%). Proof that the cloned genomic fragment corresponded to the *CTF4* gene was obtained by integration of a *LEU2* marker and subsequent linkage analysis (see Materials and Methods).

Physical and genetic map positions of *CTF4*. The *CTF4* gene was assigned to chromosome XVI by hybridization to chromosome-sized DNA separated by pulsed-field gel electrophoresis (10). To determine the physical position of *CTF4* on chromosome XVI, we used a mapping procedure that splits the chromosome at the site of a cloned DNA segment into proximal and distal chromosome fragments (9). By using this procedure to map the *CTF4*-containing DNA, two stably maintained chromosome XVI fragments were generated, and the sizes of these chromosome fragments were determined by analysis of orthogonal-field-alternation gel electrophoresis gels. The lengths of the chromosome fragments indicated that *CTF4* was 830 kb from one end of chromosome XVI and 175 kb from the other end (summarized in Fig. 3). This is consistent with the meiotic map position of *CTF4* between *KAR3* and *TEF1* (see below). We concluded that *CTF4* is localized on the right arm of chromosome XVI 175 kb from the telomere. Furthermore, the direction of transcription of *CTF4* relative to the centromere may be determined from the orientation of *CTF4* within the fragmentation vectors. *CTF4* is transcribed on chromosome XVI in the direction away from the centromere.

The *CTF4* gene was also mapped by hybridization to a gridded minimal "mapping contig" of bacteriophage λ clones on nitrocellulose filters (kindly provided by Linda Riles and Maynard Olson). The *CTF4* probe identified λ clone 5100, placing the gene on a 190-kb contig located at the right end of chromosome XVI. Clone 5100 lies 150 kb from the most telomeric segment on the contig, which is consistent with the chromosome fragmentation data.

Tetrad analyses were previously carried out to determine the position of the *CTF4* gene with respect to other mapped loci on chromosome XVI (18). Despite considerable variability of the results, it was clear that the *CTF4* gene is located between *TEF1* and *KAR3* (at 21- and 9-centimorgan distances, respectively). Finally, analysis of the sequence centromere proximal to the promoter region of *CTF4* revealed an 804-bp open reading frame which is identical to the *MSS18* gene (42). Our data therefore map the position of the *MSS18* gene, which had not been determined previously.

Sequence analysis of the *CTF4* gene. The 4.5-kb fragment of the p37 plasmid was sequenced by the Sanger dideoxy method (40). The sequence contains two open reading frames, ORF1 (804 bp) and ORF2 (2,781 bp). ORF1 is identical to the previously described *MSS18* gene (42). Deletion mapping (p37/3; Fig. 2) excluded the possibility that ORF1 was responsible for complementation of the *ctf4-1* mutation. We concluded that ORF2 corresponded to the *CTF4* gene. The nucleotide sequence of the *CTF4* gene is presented in Fig. 4; the sequence encodes a predicted protein containing 927 amino acid residues with a molecular mass of 105 kDa. The predicted primary sequence of the *CTF4* gene product was compared with both the GenBank and EMBL data bases by using the FASTP algorithm (36). No significant homologies were detected.

Analysis of the region 5′ to the *CTF4* ORF revealed the presence of a so-called *Mlu*I motif (ACGCGT) at position −122, present as a degenerate tandem repeat (ACGCG ACGCGT). The *Mlu*I motif is found upstream of many yeast genes important for DNA metabolism (see Discussion). Only 379 bp separate the stop codon of the *MSS18* gene and the initiation codon of the *CTF4* gene. Thus, the maximum length of the *CTF4* promoter is not more than 379 bp.

One of the most interesting properties of the coding region of *CTF4* is a region similar to a helix-loop-helix (HLH) motif, a structure involved in protein-protein interaction (Fig. 5). This motif has been described for a number of protein factors involved in development, cell growth, and transformation (31, 52). The HLH region is present at the C terminus of the *CTF4* protein (amino acid residues 848 to 898). Proteins with the HLH motif often also contain DNA-binding domains. We therefore searched the *CTF4* amino acid sequence for the presence of potential DNA-binding regions. The N terminus of the *CTF4* protein had three regions which might form zinc finger structures (28, 51): in positions 101 to 131 (Cys-X_2-His-X_{23}-His-X_2-His), positions 226 to 248 (Cys-X_5-

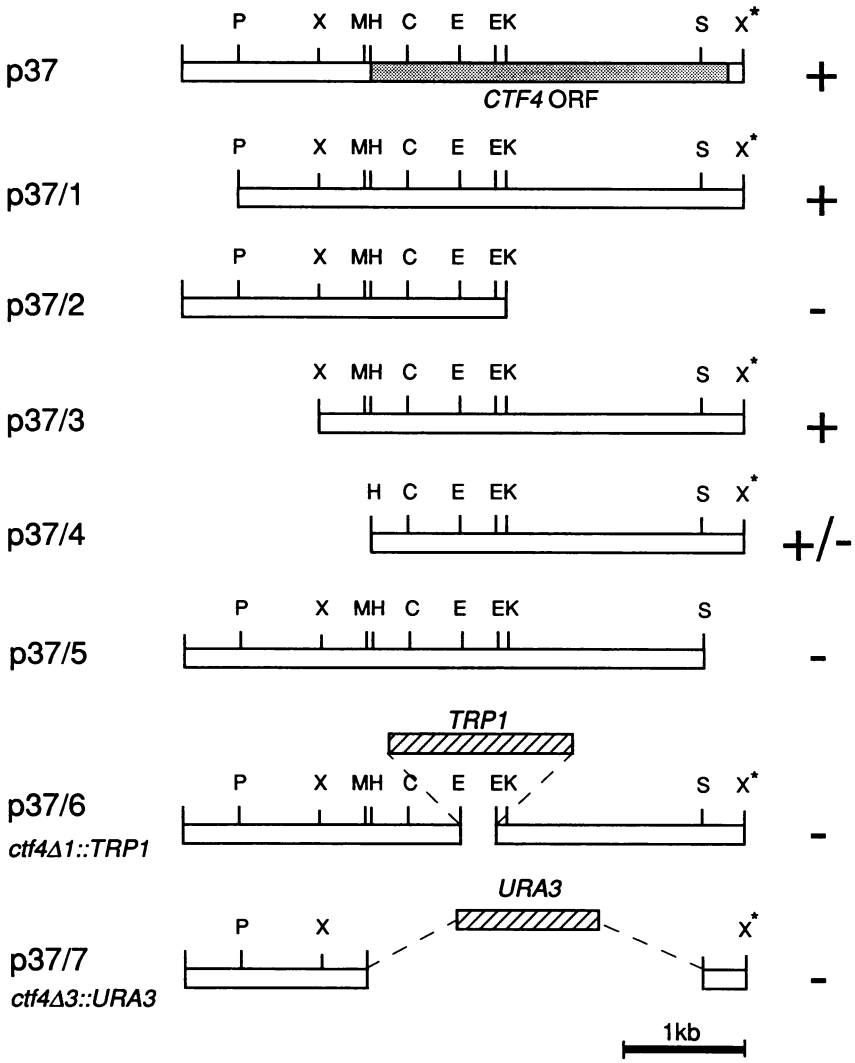

FIG. 2. Complementation analysis of subclones from the 4.5-kb genomic fragment of the p37 plasmid containing the *CTF4* gene. The restriction map of the fragment in the p37 plasmid complementing the *ctf4-1* mutation is shown. The bars beneath represent the different fragments that were subcloned into the pRS315 plasmid and tested for the presence of a functional *CTF4* gene by the ability to complement the sectoring phenotype of the *ctf4-1* mutant. + indicates complementation of the *ctf4-1* mutation. The 3.4-kb insert in p37/3 was the smallest complementing clone thus defined. Abbreviations: E, *Eco*RI; C, *Cla*I; H, *Hin*dIII; M, *Mlu*I; P, *Pst*I; S, *Sph*I; K, *Kpn*I; X, *Xba*I (not all *Xba*I sites are indicated). X* corresponds to the *Xba*I site in the polylinker of the pRS315 plasmid.

Cys-X_{10}-His-X_4-Cys), and positions 450 to 462 (His-X_2-His-X_5-His-X_2-His). The last region is similar to the structure found in single-stranded DNA-binding protein (48). The second region is reminiscent of the structures participating in recognizing the nucleotide sequences of double-stranded DNA and RNA (28). In addition, we also found 11 regions meeting the predicted requirements for coding the HTH structure (44), a protein motif commonly observed to function in sequence-specific DNA site recognition. The potential HTH positions are positions 73 to 95, 95 to 117, 126 to 148, 137 to 159, 262 to 284, 318 to 340, 320 to 342, 450 to 472, 669 to 691, 851 to 873, and 866 to 888.

Another interesting feature of the *CTF4* gene product is the presence of clusters of negatively charged amino acids in positions 112 to 126 (−8), 175 to 224 (−14), 376 to 408 (−11), 428 to 441 (−9), 799 to 826 (−11), and 836 to 854 (−6). It is known that such regions can be used for activation of transcription (24, 47). In addition to acidic regions, the *CTF4* protein contains clusters of positively charged residues at positions 317 to 326 (+4), 423 to 425 (+4), and 648 to 653 (+4). It is interesting that the first region overlaps with two regions, answering the requirements for the formation of the HTH supersecondary structure in positions 318 to 340 and 320 to 342.

The C-terminal region of the *CTF4* gene product carrying the HLH domain is essential for its function. Taking into account the important role of the HLH structure in eukaryotic regulatory proteins, we have analyzed the consequence of a mutation that deletes this structure from the *CTF4* protein. The predicted α-helix 2 of the HLH is located at the most C-terminal amino acid residues of the *CTF4* protein (Fig. 5). A unique *Sph*I site is located in the middle of the predicted loop between the two predicted helices. A 4-bp deletion was introduced at the *Sph*I site in plasmid p37. The

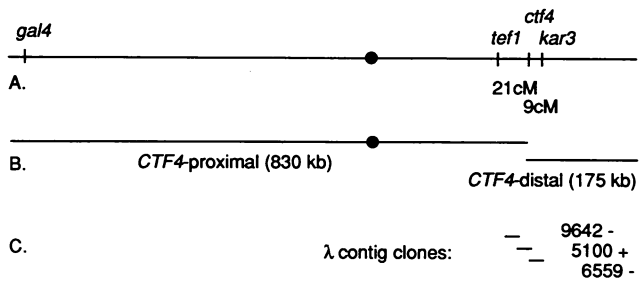

FIG. 3. Genetic and physical map positions of *CTF4*. (A) Meiotic mapping data for the *CTF4* gene came from several hybrids (18). In most cases, integrated copies of either *LEU2* or *URA3* were used. The existence of the additional DNA fragments may have affected recombination distance, especially within a small region. (B) Chromosome fragmentation at *CTF4* yielded proximal and distal fragments of the indicated sizes. (C) Hybridization of a *CTF4* probe to the genomic mapping contig of Riles and Olson resulted in one positive grid position (5100). The two nearest neighbor grid positions were negative.

deletion was confirmed by sequence analysis, and the plasmid was called p37-Δ10. The deletion causes a shift of the open reading frame at the point of the mutation. A new predicted gene product of *CTF4* is shortened by 40 amino acid residues, and the last 15 amino acids residues are absolutely different because of a shift of the open reading frame. The mutation introduced into the *CTF4* gene completely excludes the formation of HLH domain because the C-terminal amino acid residues are not capable of forming an α-helix.

Mutant plasmid p37-Δ10 was tested for the ability to complement the *ctf4-1* mutation. The *ctf4-1* strain (YNK34) transformed by plasmid p37-Δ10 exhibited a sectoring phenotype and unstable maintenance of a centromeric plasmid indistinguishable from the strain transformed by vector alone. We conclude that the HLH domain within the C-terminal region of the *CTF4* gene product is essential for *CTF4* function.

The *CTF4* gene product is not essential for cell viability. In order to investigate the role of the *CTF4* gene product in mitotic growth, we constructed a deletion mutation *ctf4-Δ3::URA3*, leaving only 147 bp at the 3′ end of the gene. *ctf4-Δ3::URA3* was introduced into the diploid strain YPH501 by one-step gene replacement (39). Replacement of one copy of *CTF4* by the mutant allele *ctf4-Δ3::URA3* was confirmed by blot hybridization (data not shown). Four independently derived diploids heterozygous for the *CTF4* deletion were sporulated, and tetrad analysis was performed. In virtually all of the tetrads examined all four spores gave rise to growing colonies, indicating that the deletion of the *CTF4* gene does not result in the loss of cell viability.

Deletion of the *RAD52* gene leads to poor growth of the *ctf4-Δ1* mutant. Given the potential role of *CTF4* in DNA metabolism, it was interesting to check the possibility of interaction between *CTF4* and *RAD52* in the chromosome cycle. To assess the possible lethal effect of combining *ctf4* and *rad52* mutations, a *ctf4-Δ1::HIS3/CTF4 rad52Δ1::URA3/RAD52* doubly heterozygous diploid was sporulated and tetrads were dissected. Spore viability was normal, indicating that the *ctf4 rad52* double null mutant was viable. However, the double mutant (Ura^+ His^+) spore clones grew very poorly compared with the wild type or either single mutant alone.

Single division pedigree analysis was performed to determine the effects of the *ctf4* and *rad52* mutations on cell viability. Four near-isogenic strains (*CTF4 RAD52*, *CTF4 rad52*, *ctf4 RAD52*, and *ctf4 rad52*) were analyzed for the cell viability of mother-daughter pairs following cell division (Table 4). Single cells were micromanipulated to defined positions on agar plates and incubated for 2 to 4 h at 30°C, and mother-daughter pairs were physically separated following the first cell division and allowed to form colonies for 2 days at 30°C. In wild-type cells, 5 of 109 cell divisions scored (5%) resulted in an inviable mother or daughter cell product; none resulted in two inviable products. A similar high frequency of viability was observed with the *rad52* mutant. In the *ctf4* mutant, 16% of the cell divisions resulted in one, and 5% resulted in two, inviable cell product(s). Thus, 14% of the cell division products are inviable in the *ctf4* mutant, compared with 1 to 2% for the wild type or the *rad52* mutant. In the *ctf4 rad52* double mutant, the effect of *ctf4* on cell viability was significantly enhanced. Thirty-two percent of the cell divisions resulted in one, and 32% of cell divisions resulted in two, inviable cell product(s), corresponding to a total value of 49% inviability following cell division. We conclude that the *RAD52* gene product is important for cell viability in a *ctf4* mutant background.

***ctf4* mutants exhibit G2/M accumulation.** Asynchronous cultures of *ctf4-Δ1::TRP1* and *CTF4* haploid strains were examined for cell cycle distribution by using flow cytometry and cell morphology. The flow cytometry profiles clearly demonstrate an accumulation of cells with 2 N DNA content in the *ctf4* mutant (Fig. 6). The *ctf4* mutant also exhibited a marked accumulation of large budded cells with a single chromosomal mass protruding into the neck (Fig. 6). Quantitation of this phenotype showed that: 1 in 300 (0.3%) of *CTF4* cells (in YPH927) and 87 of 313 (22%) of *ctf4* cells (in YPH937) exhibited the scored morphology. These results are in agreement with similar observations by Miles and Formosa (27), who performed similar analyses in a different laboratory yeast background.

DISCUSSION

The *CTF4* (*CHL15*) gene was identified in separate mutageneses (17, 46) designed to identify genes involved in mitotic chromosome transmission. Miles and Formosa (27) describe cloning and characterization of the *POB1* gene, which is identical to *CTF4*. The *POB1* gene was cloned by the criterion of encoding a protein which binds to yeast DNA polymerase α in vitro. This observation and the analysis of phenotypes associated with mutations in this gene, taken together, support the conclusion that the protein encoded by *CTF4* functions in DNA metabolism. The fact that *CTF4* is not essential for mitotic growth indicates that this gene product either performs a redundant essential function (which can also be performed by another gene product or which can be bypassed in a parallel pathway) or is required for the fidelity of a process in DNA metabolism such as DNA synthesis, recombination, or repair.

Mutations in *CTF4* lead to chromosome destabilization in mitosis. The increase in frequency of chromosome loss was observed for linear chromosomes (including natural chromosome III and chromosome fragments derived from chromosomes III and VII) as well as for circular artificial minichromosomes. The analysis of segregation of circular artificial minichromosome YCp41 and chromosome fragments showed that the loss of these structures in mitotic divisions is not accompanied by their accumulation in a part of the cell

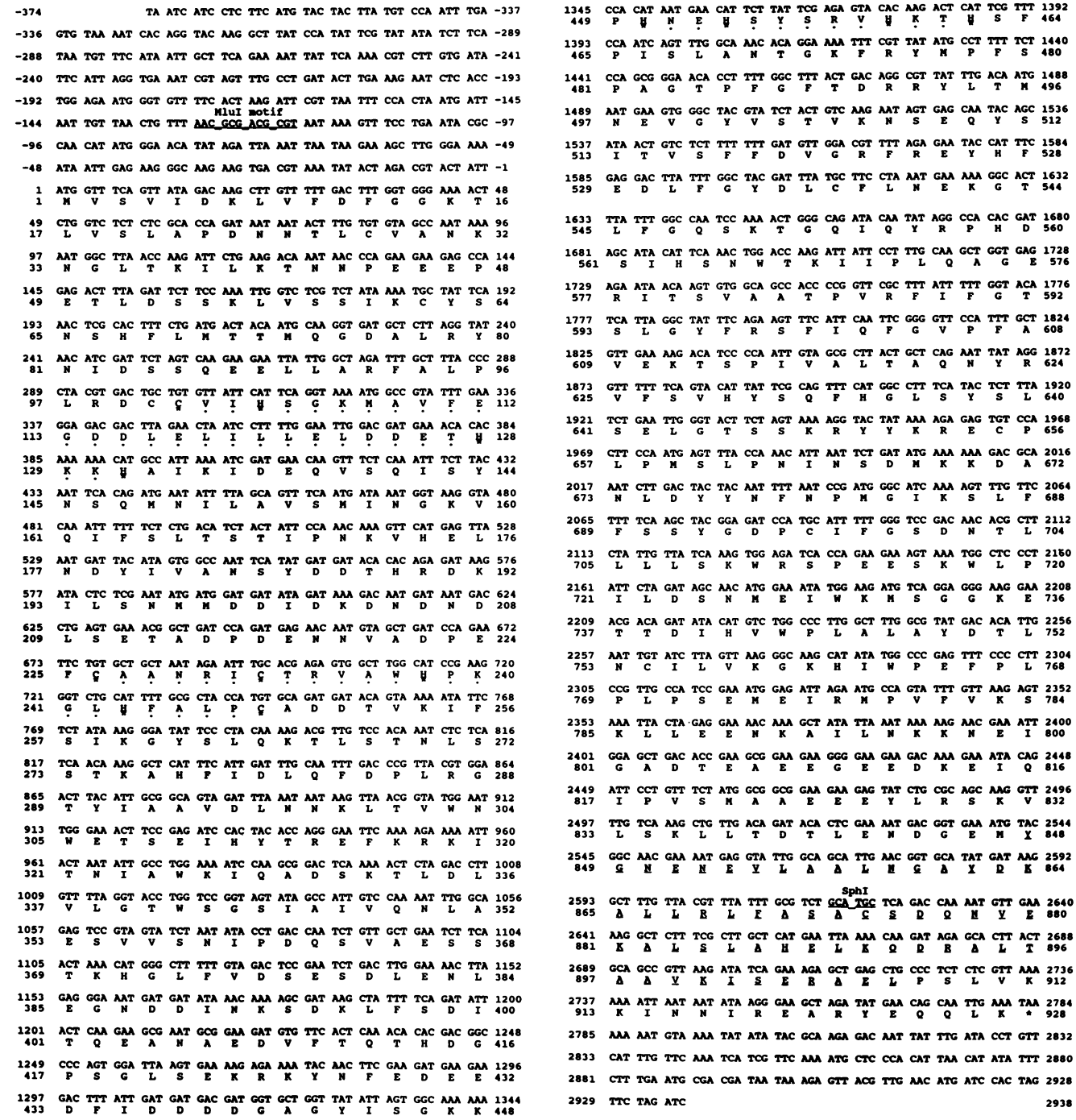

FIG. 4. Nucleotide sequence of *CTF4*. The predicted amino acid sequence, in single-letter code, is given below the nucleotide sequence. Numbers above and below each line indicate nucleotide and amino acid residues, respectively. The putative regulatory sequence ACGCGT at nucleotide −122 is underlined, as is the amino acid sequence at residues 848 to 899 which corresponds to the HLH motif. Asterisks indicate the positions of putative zinc fingers.

population. Therefore, chromosome destabilization is caused predominantly by the loss of sister chromatids rather than by nondisjunction. It has been proposed that this mode of chromosome destabilization is consistent with the presence of a defect in DNA metabolism (11, 35). The observed increase in the frequency of mitotic recombination events also supports this conclusion. An increase in mitotic recombination has been described for several DNA metabolism mutants in yeasts, including defects in DNA ligase and DNA polymerase (11).

An interesting characteristic of the *CTF4* gene is the presence of an *Mlu*I motif (degenerate repeat ACGCGT) in the promoter region, 122 bp upstream of the translational initiation codon. *Mlu*I motifs have been found in the pro-

```
                    Helix 1          Loop          Helix 2
                  1234567890123456              123456789012345678
E47      Human    VRDINEAFRELGRMCQ----MHLK---SDKAQTKLLILQQAVQVILGLEQQ
Myo D    Mouse    LSKVNEAFETLKRCTS----SNP-----NQRLPKVEILRNAIRYIEGLQAL
L myc    Human    RNDLRSRFLALRDQVP----TLAS----CSKAPKVVILSKALEYLQALVGA
CBF1     Yeast    RENINTAINVLSDLLP-----------VRESSKAAILARAAEYIQKLKET
                              |                 |  ||  |       |
consensus                     L                 K  IL  A       L
                              |                 |   |          |
CTF4     Yeast    YGNENEVLAALNGAYDKALLRLFASACSDQNEVKALSLAHELKQDRALTAA
```

FIG. 5. Sequence comparison of the HLH motif between *CTF4* and other known HLH sequences. The *CTF4* HLH motif is compared with the HLH sequences of *E47* (52), *MyoD* (31), *L-myc* (21), and yeast *CBF1* (3).

TABLE 4. Viability and one-generation pedigree analysis

Strain	Relevant genotype	No. of mother-daughter pairs dissected	No. (%) with mother or daughter dead	No. (%) with both cells dead	Inviability (%) per cell division product
YPH927	*CTF4 RAD52*	109	5 (5)	0	2
YPH936	*CTF4 rad52*	76	2 (3)	0	1
YPH937	*ctf4 RAD52*	37	6 (16)	2 (5)	14
YPH938	*ctf4 rad52*	37	12 (32)	12 (32)	49

moter regions of many genes involved in DNA metabolism in yeasts. To date, more than 20 genes of this group have been identified, including the DNA polymerase I, II, and III genes (2, 16, 29); the DNA ligase gene (54); and other genes controlling DNA replication or the synthesis of nucleotide precursors (54). The expression of these genes appears to be coordinately regulated, occurring near the boundary between the G_1 and S phases (23). The presence of the *Mlu*I motif in the promoter region of the *CTF4* gene suggests that this gene is a member of a family of genes involved in DNA metabolism. It is unknown whether the *CTF4* gene is expressed near the G_1-S boundary, as are several other genes containing the *Mlu*I motif. If *CTF4* gene expression is regulated during the cell cycle via the *Mlu*I motif, this condition apparently is not necessary for *CTF4* function. Deletion of the promoter region of this gene including the *Mlu*I motif does not destroy the ability of plasmid p37/4 to complement the *ctf4-1* mutation.

Results of double mutant studies are also consistent with a role for the *CTF4* gene product in DNA metabolism. We observed that in a *ctf4 rad52* double null mutant, the modest cell inviability phenotype caused by the *ctf4-1* mutation alone was markedly enhanced by the presence of the *rad52* mutation. Mutations in the *RAD52* gene are characterized by a pleiotropic phenotype including an increased frequency of spontaneous mutagenesis, suppression of homologous recombination, and defects in DNA double-strand break repair (30, 38). It is possible that the *ctf4-1* mutation leads to the accumulation of double-stranded breaks and/or other chromosomal lesions not reparable in *rad52* mutants. The morphology of *CTF4*-deleted cells suggests that this mutant experiences difficulty progressing from S phase into mitosis, similar to known DNA metabolism mutants. It is interesting, however, that the observed G2 accumulation in *ctf4*-defective cells is not affected in a *ctf4 rad9* double mutant (27). These data suggest that if chromosomal lesions are accumulating in a *ctf4* mutant, they are different from those induced in *cdc9* (DNA ligase) mutants or by X irradiation which are recognized by the *RAD9*-dependent mechanism of cell cycle arrest (53).

Analysis of the nucleotide sequence of the *CTF4* gene revealed the presence of a 2.8-kb open reading frame encoding a 105 kDa predicted protein. In the N-terminal region of the *CTF4* gene product, three potential zinc finger DNA-binding domains were found. Analysis of the amino acid sequence of the *CTF4* gene product revealed 11 regions as potential HTH DNA-recognizing structures (44). Two of

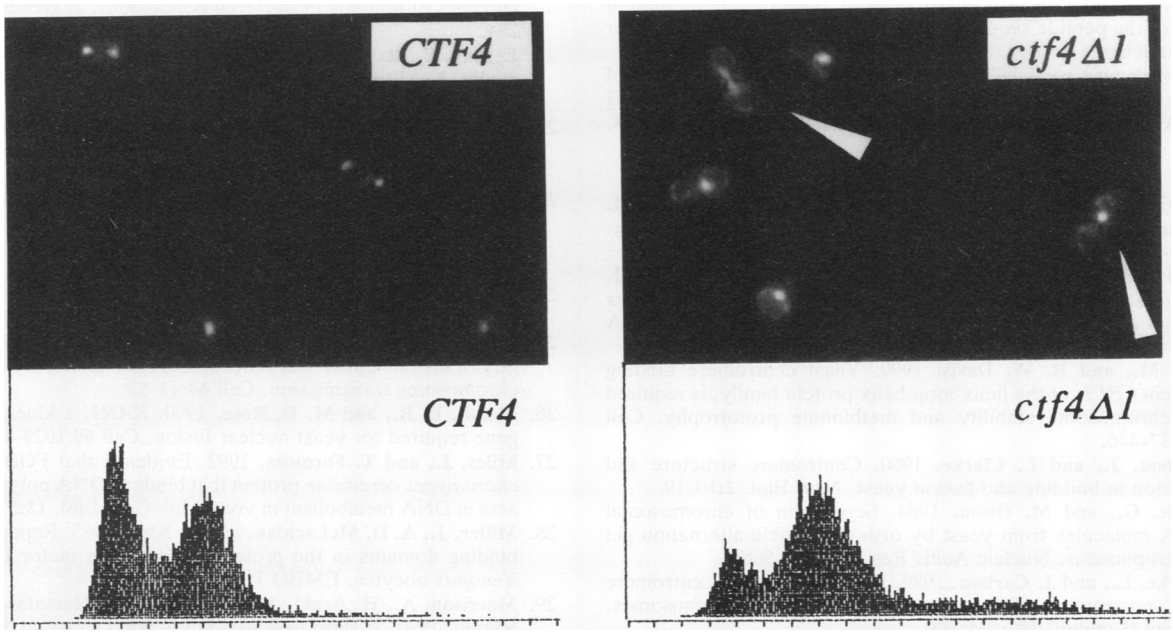

FIG. 6. Cell cycle characteristics of *ctf4* mutants. Logarithmically growing cultures of YPH927 (*CTF4*) and YPH937 (*ctf4-Δ1*) were examined for bud morphology (upper panels) and for DNA content by fluorescent staining (lower panels). Arrowheads indicate the accumulated morphology scored in *ctf4* mutants.

them (at positions 318 to 340 and 320 to 342) overlap with a cluster of positively charged residues (at positions 317 to 326). An understanding of the functional role(s) of these domains will require further study. The C-terminal region of the *CTF4* gene product bears homology to the HLH motif recently found in several regulatory proteins, one of which is a yeast protein (3, 31, 32, 52). Apparently, this HLH domain is essential for the function of the *CTF4* protein because a small deletion that removes the helix-2 region inactivates the gene product. Since HLH domains have been shown to mediate the formation of protein-protein complexes, the *CTF4* gene product may function in the cell as a homodimer or in heterodimeric association with other proteins having an HLH structure. By analogy to other proteins of the HLH family, the *CTF4* gene product can be one of the regulators of the replicative cell machinery.

In summary, the molecular genetic analysis of the *CTF4* gene provides strong support for an important function in DNA metabolism. This locus has been identified on the basis of its requirement for chromosome stability in mitosis (presented here) and also as the gene encoding a protein that associates with DNA polymerase α in vitro (*POB1* [27]). The upstream *Mlu*I motif, the presence of potential Zn finger motifs and the HLH domain in the predicted polypeptide, the predominant chromosome loss (1:0) missegregation phenotype, and elevated mitotic recombination rates in mutants are all consistent with the hypothesis that the function of this gene product is important for the maintenance of chromosomal DNA. Further, the markedly elevated lethality observed with *ctf4 rad52* double mutants implies that the lack of the *CTF4* gene product leads to the accumulation of lesions not compatible with mitotic viability in the absence of *RAD52*.

ACKNOWLEDGMENTS

We thank P. Philippsen, University of Giessen, and the Deutsche Forschungsgemeinschaft (Sonderforschungsbereich 272) for support of the sequence work and C. Connelly for technical assistance. We thank M. Koryabin for genetic mapping, B. Shestopalov for help in analysis of the peptide sequence of the *CTF4* gene, and J. Flook for flow cytometry.

This work was partially supported by the Russian Academy of Sciences High Priority Advances in Genetics grant to V.L., by NIH grant CA16519, and by a grant from the Pew Memorial Trust to P.H.

REFERENCES

1. **Benezra, R., R. L. Davis, D. Lockshon, D. L. Turner, and H. Weintraub.** 1990. The protein *Id*: a negative regulator of helix-loop-helix DNA-binding proteins. Cell **61**:49–51.
2. **Boulet, A., M. Simon, G. Faye, G. A. Bauer, and P. M. J. Burgers.** 1989. Structure and function of the *Saccharomyces cerevisiae CDC2* gene encoding the large subunit of DNA polymerase III. EMBO J. **8**:1849–1854.
3. **Cai, M., and R. W. Davis.** 1990. Yeast centromere binding protein *CBF1*, of the helix-loop-helix protein family, is required for chromosome stability and methionine prototrophy. Cell **61**:437–446.
4. **Carbon, J., and L. Clarke.** 1990. Centromere structure and function in budding and fission yeast. New Biol. **2**:10–19.
5. **Carle, G., and M. Olson.** 1984. Separation of chromosomal DNA molecules from yeast by orthogonal-field-alternation gel electrophoresis. Nucleic Acids Res. **12**:5647–5664.
6. **Clarke, L., and J. Carbon.** 1980. Isolation of yeast centromere and construction of functional circular small chromosomes. Nature (London) **287**:504–509.
7. **Fangman, W. L., and B. J. Brewer.** 1991. Activation of replication origins within yeast chromosomes. Annu. Rev. Cell Biol. **7**:375–402.
8. **Feinberg, A., and B. Vogelstein.** 1983. A technique for radio labelling of DNA restriction fragment to high specific activity. Anal. Biochem. **132**:6–13.
9. **Gerring, S., C. Connelly, and P. Hieter.** 1991. Positional mapping of cloned genes by chromosome blotting and fragmentation. Methods Enzymol. **194**:57–77.
10. **Gerring, S. L., F. Spencer, and P. Hieter.** 1990. The *CHL1 CTF1* gene product of *Saccharomyces cerevisiae* is important for chromosome transmission and normal cell cycle progression in G2/M. EMBO J. **9**:4347–4358.
11. **Hartwell, L. H., and D. Smith.** 1985. Altered fidelity of mitotic chromosome transmission in cell cycle mutants of *Saccharomyces cerevisiae*. Genetics **110**:381–395.
12. **Hieter, P., C. Mann, M. Snyder, and R. W. Davis.** 1985. Mitotic stability of yeast chromosomes: a colony color assay that measures nondisjunction and chromosome loss. Cell **40**:381–392.
13. **Hoyt, M. A., T. Stearns, and D. Botstein.** 1990. Chromosome instability mutants of *Saccharomyces cerevisiae* that are defective in microtubule-mediated processes. Mol. Cell. Biol. **10**:223–234.
14. **Hutter, K. J., and H. E. Eipel.** 1978. Flow cytometrical determination of cellular substances in algae, bacteria, moulds, and yeast. Antonie van Leeuwenhoek J. Microbiol. Serol. **44**:269–282.
15. **Ito, H., Y. Fukuda, K. Murata, and A. Kimura.** 1983. Transformation of intact yeast cells treated with alkali cations. J. Bacteriol. **153**:163–168.
16. **Johnston, L. M., M. Snyder, L. M. S. Chang, R. W. Davis, and J. L. Campbell.** 1985. Isolation of the gene encoding yeast DNA polymerase I. Cell **43**:369–377.
17. **Kouprina, N., O. B. Pashina, N. T. Nikolaishwili, A. M. Tsouladze, and V. L. Larionov.** 1988. Genetic control of chromosome stability in the yeast *Saccharomyces cerevisiae*. Yeast **4**:257–269.
18. **Kouprina, N., A. Tsouladze, M. Koryabin, F. Spencer, P. Hieter, and V. Larionov.** Identification and genetic mapping of *CHL* genes controlling mitotic chromosome transmission in yeast. Yeast, in press.
19. **Larionov, V., T. Karpova, O. Pashina, G. Zhouravleva, N. Nikolaishwili, and N. Kouprina.** 1987. The stability of chromosomes in yeast. Curr. Genet. **11**:435–443.
20. **Lea, D. E., and C. A. Coulson.** 1948. The distribution of the numbers of mutants in bacterial populations. J. Genet. **49**:264–284.
21. **Legouy, E., R. DePinho, K. Zimmerman, R. Collum, G. Yancopoulos, L. Mitsock, R. Kriz, and F. W. Alt.** 1987. Structure and expression of the murine *L-myc* gene. EMBO J. **6**:3359–3366.
22. **Liras, P., J. McCusker, S. Mascioli, and J. E. Haber.** 1978. Characterization of a mutation in yeast causing nonrandom chromosome loss during mitosis. Genetics **88**:651–671.
23. **Lowndes, N. F., A. L. Johnson, and L. H. Johnston.** 1991. Coordination of expression of DNA synthesis genes in budding yeast by a cell-cycle regulated *trans* factor. Nature (London) **350**:247–250.
24. **Ma, J., and M. Ptashne.** 1987. Deletion analysis of *GAL4* defines two transcriptional activating segments. Cell **48**:847–853.
25. **Meeks-Wagner, D., and L. Hartwell.** 1986. Normal stoichiometry of histone dimer sets is necessary for high fidelity of mitotic chromosome transmission. Cell **44**:43–52.
26. **Meluh, P. B., and M. D. Rose.** 1990. *KAR3*, a kinesin-related gene required for yeast nuclear fusion. Cell **60**:1029–1041.
27. **Miles, J., and T. Formosa.** 1992. Evidence that POB1, a *Saccharomyces cerevisiae* protein that binds to DNA polymerase α, acts in DNA metabolism in vivo. Mol. Cell. Biol. **12**:5724–5735.
28. **Miller, J., A. D. McLachlan, and A. Klug.** 1985. Repetitive zinc binding domains in the protein transcription factor IIIA from *Xenopus* oocytes. EMBO J. **4**:1609–1614.
29. **Morrison, A., H. Araki, A. B. Clark, R. K. Hamatake, and A. Sugino.** 1990. A third essential DNA polymerase in *Saccharomyces cerevisiae*. Cell **62**:1143–1151.
30. **Mortimer, R. K., R. Contopoulou, and D. Schild.** 1981. Mitotic chromosome loss in a radiation-sensitive strain of the yeast

Saccharomyces cerevisiae. Proc. Natl. Acad. Sci. USA **78:** 5778–5782.
31. **Murre, C., P. S. McCaw, and D. Baltimore.** 1989. A new DNA-binding and dimerization motif in immunoglobulin enhancer binding, *daughter-less*, *MyoD* and *myc* proteins. Cell **56:**777–783.
32. **Murre, C., P. S. McCaw, H. Vaessin, M. Caudy, L. Y. Jan, N. Y. Jan, C. V. Cabrera, J. N. Buskin, S. D. Hauschka, A. B. Lassar, H. Weintraub, and D. Baltimore.** 1989. Interactions between heterologous helix-loop-helix proteins generate complexes that bind specifically to a common DNA sequence. Cell **58:**537–544.
33. **Neff, J., J. H. Thomas, P. Grisafi, and D. Botstein.** 1983. Isolation of the β-tubulin gene from yeast and demonstration of its essential function in vivo. Cell **33:**211–219.
34. **Newlon, C. S.** 1988. Yeast chromosome replication and segregation. Microbiol. Rev. **52:**568–601.
35. **Palmer, R. E., E. Hogan, and D. Koshland.** 1990. Mitotic transmission of artificial chromosomes in *cdc* mutants of the yeast, *Saccharomyces cerevisiae*. Genetics **125:**763–774.
36. **Pearson, W. R., and D. J. Lipman.** 1985. Rapid and sensitive protein similarity searches. Science **227:**1435–1441.
37. **Pirozhkov, V., A. Tsouladze, N. Kouprina, and V. Larionov.** 1984. Determination of probability of plasmid loss per generation. Gene **28:**237–239.
38. **Resnick, M. A., and P. Martin.** 1976. The repair of double-strand breaks in the nuclear DNA of *Saccharomyces cerevisiae* and its genetic control. Mol. Gen. Genet. **143:**119–129.
38a. **Riles, L., and M. V. Olson.** Unpublished data.
39. **Rothstein, R. J.** 1983. One-step gene disruption in yeast. Methods Enzymol. **101:**202–211.
40. **Sanger, F., S. Nicklen, and A. R. Coulson.** 1977. DNA sequencing with chain-terminating inhibitors. Proc. Natl. Acad. Sci. USA **74:**5463–5467.
41. **Schatz, P. J., F. Solomon, and D. Botstein.** 1986. Genetically essential and nonessential α-tubulin genes specify functionally interchangeable proteins. Mol. Cell. Biol. **6:**3722–3733.
42. **Seraphin, B., M. Simon, and G. Faye.** 1988. *MSS18*, a yeast nuclear gene involved in the splicing of intron a*15*β of the mitochondrial *COX1* transcript. EMBO J. **7:**1455–1464.
43. **Sherman, F., G. R. Fink, and C. W. Lawrence.** 1979. Methods in yeast genetics. Cold Spring Harbor Laboratory, Cold Spring Harbor, N.Y.
44. **Shestopalov, B. V.** 1988. Amino acid sequence template useful for α helix-turn-α helix prediction. FEBS Lett. **233:**105–108.
45. **Sikorski, R. S., and P. Hieter.** 1989. A system of shuttle vectors and yeast host strains designed for efficient manipulation of DNA in *Saccharomyces cerevisiae*. Genetics **122:**19–27.
46. **Spencer, F., S. L. Gerring, C. Connelly, and P. Hieter.** 1990. Mitotic chromosome transmission fidelity mutants in *Saccharomyces cerevisiae*. Genetics **124:**237–249.
46a. **Spencer, F., and P. Hieter.** Unpublished data.
47. **Struhl, K.** 1987. Promoters, activation proteins, and the mechanism of transcriptional initiation in yeast. Cell **49:**295–297.
48. **Summers, M. F.** 1991. Zinc finger motif for single-stranded nucleic acids? J. Cell. Biochem. **45:**41–48.
49. **Sung, P., L. Prakash, W. S. Matson, and S. Prakash.** 1987. The *RAD3* gene of *Saccharomyces cerevisiae* encodes a DNA-dependent ATPase. Proc. Natl. Acad. Sci. USA **84:**8951–8955.
49a. **Truehart, J.** Unpublished data.
50. **Tschumper, G., and J. Carbon.** 1980. Sequence of a yeast DNA fragment containing a chromosome replicator and the *TRP1* gene. Gene **10:**157–166.
51. **Valee, B. L., J. E. Coleman, and D. S. Auld.** 1991. Zinc fingers, zinc clusters and zinc twists in DNA-binding protein domains. Proc. Natl. Acad. Sci. USA **88:**999–1003.
52. **Voronova, A., and D. Baltimore.** 1990. Mutations that disrupt DNA binding and dimer formation in the *E47* helix-loop-helix protein map to distinct domains. Proc. Natl. Acad. Sci. USA **87:**4722–4726.
53. **Weinert, T. A., and L. Hartwell.** 1988. The *RAD9* gene controls the cell cycle response to DNA damage in *Saccharomyces cerevisiae*. Science **241:**317–322.
54. **White, J. H. M., S. R. Green, D. G. Barker, L. B. Dumas, and L. B. Johnston.** 1987. The *CDC8* transcript is cell cycle-regulated in yeast and is expressed coordinately with *CDC9* and *CDC21* at a point preceding histone transcription. Exp. Cell Res. **171:**223–231.
55. **Zakian, V. A.** 1989. Structure and function of telomeres. Annu. Rev. Genet. **23:**579–604.